Prediction performance of linear models and gradient boosting machine on complex phenotypes in outbred mice

B.C. Perez[1], M.C.A.M. Bink[1], G.A. Churchill[2], K.L. Svenson[2], M.P.L. Calus[3]

[1] *Hendrix Genetics B.V., Research and Technology Center (RTC), P.O. Box 114, 5830 AC Boxmeer, the Netherlands.*
[2] *The Jackson Laboratory, Bar Harbor, Maine, United States of America.*
[3] *Wageningen University & Research, Animal Breeding and Genomics, P.O. Box 338, 6700 AH Wageningen, the Netherlands.*

Corresponding author: mario.calus@wur.nl

ABSTRACT

Recent literature suggests machine learning methods can capture interactions between loci and therefore could outperform linear models when predicting traits with relevant epistatic effects. However, investigating this empirically requires data with high mapping resolution and phenotypes for traits with known non-additive gene action. The objective of the present study was to compare the performance of linear (GBLUP, BayesB and elastic net [ENET]) methods to a non-parametric tree-based ensemble (gradient boosting machine – GBM) method for genomic prediction of complex traits in mice. The dataset used contained phenotypic and genotypic information for 835 animals from 6 non-overlapping generations. Traits analyzed were bone mineral density (BMD), body weight at 10, 15 and 20 weeks (BW10, BW15 and BW20), fat percentage (FAT%), circulating cholesterol (CHOL), glucose (GLUC), insulin (INS) and triglycerides (TGL), and urine creatinine (UCRT). After quality control, the genotype dataset contained 50,112 SNP markers. Animals from older generations were considered as a reference subset, while animals in the latest generation as candidates for the validation subset. We also evaluated the impact of different levels of connectedness between reference and validation sets. Model performance was measured as the Pearson's correlation coefficient and mean squared error (MSE) between adjusted phenotypes and the model's prediction for animals in the validation subset. Outcomes were also compared across models by checking the overlapping top markers and animals. Linear models outperformed GBM for seven out of ten traits. For these models, accuracy was proportional to the trait's heritability. For traits BMD, CHOL and GLU, the GBM model showed better prediction accuracy and lower MSE. Interestingly, for these three traits there is evidence in literature of a relevant portion of phenotypic variance being explained by epistatic effects. We noticed that for lower connectedness, i.e., imposing a gap of one to two generations between reference and validation populations, the superior performance of GBM was only maintained for GLU. Using a subset of top markers selected from a GBM model helped for some of the traits to improve accuracy of prediction when these were fitted into linear and GBM models. The GBM model showed consistently fewer markers and animals in common among the top ranked than linear models. Our results indicate that GBM is more strongly affected by data size and decreased connectedness between reference and validation sets than the linear models. Nevertheless, our results indicate that GBM is a competitive method to predict complex traits in an outbred mice population, especially for traits with assumed epistatic effects.

INTRODUCTION

The use of genome-wide markers as predictor variables for individuals' unobserved phenotypes (Meuwissen et al., 2001) based on a reference population is known as genomic prediction (GP). In the past decade, high-throughput genotyping technologies made GP accessible and facilitated large-scale use of GP for animal (Boichard, 2016) and plant (Bhat et al., 2016) breeding, and in human genetics (Lappalainen et al., 2019). For animals and plants, GP has reduced breeding costs and speeded up breeding programs as individuals of interest can be selected in earlier stages of life, while reducing costs for performance testing. In humans, major efforts have been put into developing GP to score disease risks (Duncan et al., 2019), aiming for a more personalized medicine in the future (Barrera-Saldaña, 2020).

Currently, most GP models implemented assume that observed phenotypes are controlled by numerous loci with additive effects throughout the genome and this approach has provided a robust performance in most cases (Meuwissen et al., 2001; Calus, 2010). However, in the literature it has been suggested that the genetic architecture of complex traits may involve significant proportions of non-additive genetic (dominance or epistasis) effects (Mackay, 2014) and that these could be much more common than previously thought (Sackton and Hartl, 2016). Although accounting for non-additive effects into parametric GP models has been reported to improve predictive performance (Forsberg et al., 2017) of phenotypes, implementing variable selection to prioritize among all possible SNP by SNP interactions, is computationally too costly for any practical application.

Machine learning (ML) has been successfully used in many fields for text, image and audio processing at huge data volumes. Recently, these algorithms have found many applications in GP for offering an opportunity to model complex trait architectures in a much simpler framework than parametric models (Nayeri et al. 2019; Montesinos-López et al., 2021; van Dijk et al., 2021). ML algorithms are free from model specification, can accommodate interactions between predictive variables and deal with large numbers of

predictor variables by performing automatic variable selection (Jiang et al., 2009; Li et al., 2018).

Howard et al. (2014), Ghafouri-Kesbi et al. (2015) and Abdolahi-Arpanahi et al. (2020) have compared the predictive performance of linear and ML models for simulated phenotypes controlled by additive or non-additive effects. In general, linear models were able to outperform ML models for traits controlled by additive effects, however they failed to do so when used to predict traits with purely epistatic architecture. The superiority of ML over traditional linear models was markedly observed for traits controlled by a low number of loci (100) with non-additive effects. For this type of scenario, Ghafouri-Kesbi et al. (2015) and Abdolahi-Arpanahi et al. (2020) also showed a consistent good performance of the gradient boosting machine (GBM) algorithm (Friedman, 2001), which has previously been reported to provide robust predictive ability when compared to other methods in the context of GP (González-Recio et al., 2011, 2013, 2014; Ogutu et al., 2011; Jimenez-Montero et al., 2013; Grinberg et al., 2019; Srivastava et al., 2021).

Although results in simulated data suggest the superiority of ML models in the presence of epistatic effects, the performance of such models have been much less consistent for GP using real datasets. Zingaretti et al. (2020) observed that convolutional neural networks (CNN) had 20% higher predictive accuracy than linear models for GP of a trait with a strong dominance component (percentage of culled fruit) in strawberry but underperformed for traits with predominant additive effects. On the other hand, in Azodi et al. (2019), ML did not consistently outperform linear models for traits with strong evidence of underlying non-additive architectures (for example height in maize and rice). The authors also describe that ML models presented less stable prediction across traits than linear models. Similar results were also reported by Bellot et al. (2018) while investigating the performance of GP for several complex human phenotypes. An important aspect to consider when investigating performance of GP models is that for most livestock and plant species there is currently limited knowledge over the genetic architecture of economically interesting

traits. This makes it difficult to perform inference about the real reasons why ML outperforms linear models in specific situations. This could be overcome by considering data from populations for which knowledge on genetic architecture of traits is more extensively and accurately described.

The Diversity Outbred (DO) mice population is derived from eight inbred founder strains (Svenson et al. 2012). It is an interesting resource for high-resolution genetic mapping by having a low level of genetic relationship between individuals, low extent of LD (Churchill et al., 2012) and uniformly distributed variation across genomic regions of known genes (Yang et al., 2011). This structure represents an advantage over classical inbred strains of mice or livestock populations, which have limited genetic diversity (Yang et al. 2011). These aspects allow the investigation of relevant traits in a structured scheme that closely reflects the genetic mechanisms of human disease (Churchill et al., 2012, Svenson et al., 2012).

In the present study, the objective was to compare performance of GBM to several linear models (GBLUP, BayesB and elastic net) for predicting ten complex phenotypes in the DO mice population. All models were applied for scenarios where data was not available for one or more generations in between the reference and validation sets. Additionally, we explore the use of feature selection from the GBM algorithm as a tool for sub-setting relevant markers and to improve prediction accuracy through dimensional reduction.

MATERIAL AND METHODS

Data

Phenotypes

The DO mice dataset comprising 835 animals was obtained from The Jackson Laboratory (Bar Harbor, ME). The animals originated from 6 non-overlapping generations (4, 5, 7, 8, 9 and 11) in which males and females were represented equally. The total number of animals per generation was 97, 48, 200, 184, 99 and 197 for generations 4, 5, 7, 8, 9, and

11, respectively, but numbers of missing records varied across traits (Figure 1). The mice were maintained on either standard high fiber (chow, n=446) or high fat diet (HFD; n=389) from weaning until 23 weeks of age. The proportion of males and females within each diet category was close to 50-50 for all generations. The same was observed for the frequency of males and females within each litter-generation combination (two litters per generation). A detailed description of husbandry and phenotyping methods can be found in Svenson et al. (2012).

Table 1 shows a comprehensive description of each trait regarding dataset size, estimated heritability and assumed genetic architecture with associated literature. Among all phenotypes available we chose 10 traits based on their distinct assumed genetic architectures from previous results with the same dataset (Li and Churchill, 2010; Churchill et al.,2012; Zhang et al., 2012; Tyler et al.,2016, 2017; Keller et al., 2019; Keenan et al., 2021) and other populations (Chitre et al., 2018). The analyzed traits were bone mineral density at 12 weeks (BMD), body weight at 10, 15 and 20 weeks (BW10, BW15 and BW20); circulating cholesterol at 19 weeks (CHOL), adjusted body fat percentage at 12 weeks (FATP), circulating glucose at 19 weeks (GLU), circulating triglycerides at 19 weeks (TRGL), circulating insulin at 8 weeks (INSUL) and urine creatinine at 20 weeks (UCRT). These traits can be categorized into measurements of body composition (weights and fat percentage), clinical plasma chemistries (triglycerides, glucose, insulin) and urine chemistry (urine creatinine).

Prior to any analyses performed in this study, phenotypic records were pre-corrected for fixed effects of diet, generation, litter and sex. The pre-corrected phenotype (y^*) can be represented by:

$$\boldsymbol{y}^* = \boldsymbol{a} + \boldsymbol{e}$$

where $\boldsymbol{a}$ is the vector of animal additive genetic effects and $\boldsymbol{e}$ the vector of residuals.

153

154 **TABLE 1**

155

156 *Genotypes*

157 Mice from 8 distinct founder strains were genotyped using either the MUGA and
158 MegaMUGA SNP arrays (Morgan et al. 2016). The variant calls from the arrays in the
159 animals contained in the current dataset were converted to founder haplotypes using a
160 hidden Markov model (HMM) (Gatti et al. 2014), which uses the order of SNPs in an
161 individual mouse to infer transition points between different DO founder haplotypes. After
162 that, the probability of each parental haplotype at each SNP position in the genome (Gatti et
163 al., 2014) was used to derive SNP genotype probabilities. To accomplish that, we used
164 functions available in the "QTL2" R package (Broman et al. 2018). The complete genotype
165 file used for the analyses was composed of 64,000 markers reconstructed from the diplotype
166 probabilities from the MUGA and MegaMUGA on an evenly spaced grid, and the average
167 distance between markers was 0.0238 cM. The full genotype data (64K markers) was
168 cleaned based on the following criteria: variants with minor allele frequency < 0.05, call rates
169 < 0.90 and linear correlation between subsequent SNPs > 0.98 were removed. After quality
170 control, a total of 52,840 SNP markers were available for the mice with both phenotypic and
171 genotypic records.

172

173 ***Genomic prediction models***

174 ***GBLUP***

175 The statistical model of GBLUP is:

$$\mathbf{y}^* = \mathbf{1}\mu + \mathbf{a} + \mathbf{e},$$

176 where $\mathbf{y}^*$ is the vector of pre-corrected phenotypes, $\mathbf{1}$ is a vector of ones, μ is the
177 intercept, $\mathbf{a}$ is the vector of random additive genetic values, where $\mathbf{a} \sim N(\mathbf{0}, \mathbf{G}\sigma_a^2)$ and $\mathbf{G}$ is the

additive genomic relationship matrix between genotyped individuals. It is constructed following the second method described by VanRaden (2008) as $\frac{\mathbf{ZZ}'}{m}$ where $\mathbf{Z}$ is the matrix of centered and standardized genotypes for all individuals and m is the number of markers, and σ_a^2 is the additive genomic variance, $\mathbf{e}$ is the vector of random residual effects where $\mathbf{e} \sim N(\mathbf{0}, \mathbf{I}\sigma_e^2)$ with σ_e^2 being the residual variance, and $\mathbf{I}$ is an identity matrix. GBLUP was implemented using a Bayesian approach using the BGLR package (Pérez and de los Campos, 2014). The Gibbs sampler was run for 150,000 iterations, with a 50,000 burn-in period and a thinning interval of 10 iterations. Consequently, inference was based on 10,000 posterior samples.

BayesB

BayesB has been widely used for genomic prediction (Meuwissen et al., 2001), and here we considered it for being a linear model with variable selection ability. The phenotype of the i^{th} individual is expressed as a linear regression on markers:

$$\mathbf{y}^* = \mathbf{1}\mu + \boldsymbol{Z\beta} + \boldsymbol{e}\ ,$$

where $\mathbf{y}^*$ is the vector of pre-corrected phenotypes, $\mathbf{1}$ is a vector of ones, μ is the intercept, $\boldsymbol{\beta}$ is the vector of random effect of markers, $\boldsymbol{Z}$ is the incidence matrix for markers and $\boldsymbol{e}$ is a random residual where $\mathbf{e} \sim N(\mathbf{0}, \mathbf{I}\sigma_e^2)$ with σ_e^2 being the residual variance, and $\mathbf{I}$ is an identity matrix. Contrary to GBLUP, BayesB assumes *a priori* that all markers do not contribute to genetic variation equally. For BayesB, all markers are assumed to have a two-component mixture prior distribution. Any given marker has either a null effect with known prior probability, π, or a t prior distribution with probability $(1 - \pi)$, with ν degrees of freedom and scale parameter s^2. Therefore, marker effects $\boldsymbol{\beta} \sim N(0, \sigma_{gk}^2)$, where σ_{gk}^2 is the variance of the k^{th} SNP effect. The BayesB model was implemented using the BGLR package (Pérez and de los Campos, 2014). The Gibbs sampler was run for 120,000

iterations, with a 20,000 burn-in period and a thinning interval of 100 iterations. Consequently, inference was performed based in 10,000 posterior samples.

Elastic Net

The elastic net (ENET) is an extension of the lasso (Friedman et al., 2010) and is considered a robust method under the presence of strong collinearity among predictors, as is the case for genotype data. It can be described by the regression model:

$$\mathbf{y}^* = \boldsymbol{Z\beta} + \boldsymbol{e}\ ,$$

where $\mathbf{y}^*$ is the vector of pre-corrected phenotypes, $\boldsymbol{\beta}$ is the vector of random effect of markers, $\boldsymbol{Z}$ is the incidence matrix for markers and $\boldsymbol{e}$ is a random residual where $\mathbf{e} \sim N(\mathbf{0}, \mathbf{I}\sigma_e^2)$ with σ_e^2 being the residual variance, and $\mathbf{I}$ is an identity matrix..

The ENET uses a mixture of the ℓ_1 (lasso) and ℓ_2 (ridge regression) penalties and the estimator $\widehat{\boldsymbol{\beta}}_{ENET}$ can be formulated as:

$$\widehat{\boldsymbol{\beta}}_{ENET} = \left(1 + \frac{\lambda_2}{n}\right)\{argmin_{\boldsymbol{\beta}}\ \|\boldsymbol{y} - \boldsymbol{X\beta}\|_2^2 + \lambda_2\ \|\boldsymbol{\beta}\|_2^2 + \lambda_1\|\boldsymbol{\beta}\|_1\},$$

where $\|\boldsymbol{\beta}\|_1 = \sum_{j=1}^{p} |\boldsymbol{\beta_j}|$ is the ℓ_1- norm penalty on $\boldsymbol{\beta}$, $\|\boldsymbol{\beta}\|_2^2 = \sum_{j=1}^{p} \boldsymbol{\beta_j^2}$ is the ℓ_2- norm penalty on $\boldsymbol{\beta}$, $\|\boldsymbol{y} - \boldsymbol{X\beta}\|_2^2 = \sum_{i=1}^{n}(\boldsymbol{y}_i - \boldsymbol{x}_i^T\boldsymbol{\beta})^2$ is the ℓ_2- norm (quadratic) loss function (residual sum of squares), x_i^T is the i-th row of $\boldsymbol{X}$, λ_1 is the parameter that controls the extent of variable selection and λ_2 is the parameter that regulates the strength of linear shrinkage.

When setting $\alpha = \frac{\lambda_2}{(\lambda_1 + \lambda_2)}$, the ENET estimator is equivalent to the minimizer of:

$\widehat{\boldsymbol{\beta}}_{ENET2} = argmin_{\boldsymbol{\beta}}\ \|\boldsymbol{y} - \boldsymbol{X\beta}\|_2^2$, subject to $P_\alpha(\boldsymbol{\beta}) = (\mathbf{1} - \alpha)\|\boldsymbol{\beta}\|_1 + \alpha\|\boldsymbol{\beta}\|_2^2 \leq s$ for some s

where $P_\alpha(\boldsymbol{\beta})$ is the ENET penalty (Zou and Hastie, 2005). The ENET is equivalent to ridge regression (Hoerl and Kennard, 1970) when $\alpha = 1$, and to the lasso when $\alpha = 0$. In practice,

the ℓ_1 component performs automatic variable selection while the ℓ_2 component ensures that a group of highly correlated variables get effect estimates of similar magnitude.

We implemented the ENET model using the h2o.ai R package (Click et al. 2016). To establish the best hyperparameter set for ENET, we performed a cross-validation (splitting the reference set into 80-20 for train/test sets, as depicted in Figure 1) on a two-step scheme. First a grid search of values for the parameter α considering from 0 to 1, in intervals of 0.05. For tested value of α, the best value of λ was obtained by computing models sequentially, starting with $\lambda = 1$ and decreasing it exponentially until 0.01 in up to 20 steps. For each analysis, the best ENET model was chosen by the combination of α and λ parameters obtained from the grid search that yielded the lowest mean squared error of prediction in the test set, and this model was used to predict the validation animals (Supplementary Material - Figure S1).

Gradient Boosting Machine

Gradient boosting machine (GBM) is an ensemble learning technique that applies an iterative process of assembling “weak learners” into a stronger learner, being largely used for both classification and regression problems (Friedman, 2002;). It relies on fitting decision trees as the base learner (Hastie et al., 2009). The first tree is fitted on the errors of an initialized prediction based on the distribution of the response variable and from this point, the algorithm fits sequential trees, in which every subsequent tree aims to minimize the prediction error from the previous one until no further improvement can be achieved. Many different parameters can be used to measure that “improvement”, in the present study we used the mean squared error (MSE). GBM does automatic feature selection, prioritizing important variables and discarding ones containing irrelevant or redundant information. We implemented the GBM model using the h2o.ai R package (Click et al. 2016).

The performance of machine learning methods can be sensitive to hyper-parameters (Azodi et al., 2019). To obtain the best possible results from the GBM algorithm, a grid

search approach was used to determine the combination of hyperparameters that maximized prediction performance for each trait. Hyperparameters (and range of values) included were number of trees (*ntree* = 100, 150, 200, 300, 500, 1000, 2000 and 5000), learning rate (*lrn_rate* = 0.01; 0.05 and 0.10) and maximum tree depth (*max_depth* = 2, 3, 5 and 10). For each trait analyzed, the hyperparameter tuning scheme was performed inside the reference subset (cf. ENET and Figure 1). The best set of hyperparameters was chosen based on the lowest mean squared error obtained from the grid-search. Results reported in the present study for GBM model refer to the best performing model out of the grid search for each trait (Supplementary Material - Figure S1).

Model performance

Performance of predictions from the models was measured by the accuracy, computed as the Pearson correlation ($r_{y^*,\hat{y}}$), and the mean squared error of prediction (MSE) between predicted ($\hat{y}$) and pre-corrected phenotypes (y^*): MSE = $\frac{1}{n}\sum_{i=1}^{n}(y^* - \hat{y})^2$. In all analyses, we used a forward prediction validation scheme in which animals from older generations (4, 5, 7, 8 and 9) were used as the reference and animals from the younger generation (11) as the validation subset. Uncertainties around the $r_{y^*,\hat{y}}$ estimates were obtained by using bootstrapping (Davison and Hinkley, 1997), implemented in the “boot” R package (Canty and Ripley, 2021).

FIGURE 1

Impact of the distance between a fixed-size reference and the validation set

Here we tested the impact of an increase in distance between the reference and validation sets on the prediction performance of each model. To accomplish that, we considered 3 scenarios using generation 11 as validation as before: Using generations 4, 5, 7, 8 and 9 as reference (NoGAP), using generations 4, 5, 7 and 8 as reference and omitting phenotypes from generation 9 (GAP9), using generation 4, 5 and 7 as reference and omitting phenotypes from generations 8 and 9 (GAP8+9). Considering the full dataset there were in total 638 animals from generations 4 to 9 available to be sampled for the validation subset. To analyze the proposed scenarios, the number of animals sampled for the reference subset was kept the same in all scenarios (N=300), with a constraint on the number of animals sampled from each generation to match its representativeness in NoGAP scenario (Supplementary Material - Table S2 for details). The fixed sample size of 300 was arbitrarily chosen based on the number of records available in GAP89, the scenario with the least available data to be sampled for the reference subset (N=345). Every scenario was evaluated in 20 replicates, inference was based on the average and standard deviation of accuracies obtained from replicates. All described models were applied to each of the 20 replicates (in every scenario) considering the same sampled dataset in each replicate across models. The complete list of animals sampled in each of the 20 replicates used for the analyses is provided in the Supplementary Material.

Feature importance for dimensionality reduction

For GBM, the importance of a feature is determined by assessing whether that feature was selected to split on during the tree building process, and the contribution of that to decrease the squared error (averaged over all trees) as a result (Friedman and Meulman, 2003; Hastie, Tibshirani and Friedman, 2009). The feature importance is expressed in a percentage scale that can be ranked to assess the magnitude of importance of each feature.

Here we investigate if the feature importance performed by the GBM model can be used to improve performance by fitting only extracted relevant features, i.e., SNPs, in GBM or any of the other models. We considered the top 100, 250, 500 and 1000 features from a GBM model using the cross-validation strategy previously explained as input for GBLUP, ENET and GBM models. The important features were obtained using the same strategy described for the hyperparameter tuning previously explained, thus using a random split (80-20) within the reference subset (Figure 1).

Similarities among top SNPs and prediction rankings

To assess the relationship between model's prediction at the animal level, we quantified the number of animals in common in the top 20 ranked animals (approximately top 10% of generation 11) from each model. The latter metric gives an indication of the extent to which the same animals would be selected using these different models in a breeding program where each generation 10% of the animals are selected as parents of the next generation. Also, to understand the relationship between predictions from the models at the genome level, we quantified the overlap between the top 1000 ranked SNP among the models and traits analyzed. For any given trait, an "overlapping SNP" between two models A and B was defined as any SNP in the top 1000 ranked for model A identical or in high LD (r^2 > 0.90) with a SNP among the top 1000 ranked from model B. This approach may yield different results depending on one starting the comparison from model A to model B or vice versa and, therefore, here we report results for both directions.

Data and software availability

All data associated with this manuscript can be obtained at https://figshare.com/s/8bdd723be9d0e748cadf. The code developed and used to perform

326 analyzes described in this manuscript are included as Supplementary Material, as well as a
327 detailed description of results. All software used is publicly available.

328

329 **RESULTS**

330 ***Model performance***

331 The accuracy of predicted phenotypes from GBLUP, BayesB, ENET and GBM for
332 animals in the validation set (generation 11) is shown in Figure 2. The best performing model
333 varied according to the trait being analyzed.

334 Prediction accuracies obtained for traditional linear models (GBLUP and BayesB)
335 were, in general, proportional to the trait's heritability, with GBLUP overcoming BayesB for
336 BMD, GLUC, INSUL, TRGL and UCRT. Predictive accuracy obtained with GBLUP was
337 never the worst among tested models for any of the traits. The highest prediction accuracies
338 were observed for body composition traits (BW10, BW15, BW20 and FATP), for which
339 BayesB outperformed all other models. Conversely, BayesB particularly underperformed
340 when analyzing GLUC which was one of the traits with the lowest overall accuracy across
341 linear models. The ENET had lower prediction accuracy when compared to other models
342 across traits. It was never the best performing model for a particular trait and showed the
343 worst performance for BMD, BW10, BW15, BW20, INSUL and TRGL.

344

345 **FIGURE 2**
346

347 The GBM model showed best predictive performance for BMD, CHOL and GLUC.
348 For other traits, prediction accuracy from GBM varied from being competitive to the linear
349 models for BW10, BW15 and TRGL, to a poorer performance observed for UCRT. It only
350 showed the worst predictive ability among all models for FATP, but with a small difference
351 from the next performing model (- 1.76% absolute difference). The GBM model performed
352 particularly well when analyzing GLUC, showing predictive performance much higher than

the linear models. Overall, GBM showed a less consistent pattern of predictive performance across trait categories when compared to the linear models.

In terms of prediction error, GBLUP was the model with best performance for most traits, in most cases followed by GBM. The GBM model showed the lowest MSE for BMD, CHOL and GLUC. For all traits, BayesB showed the highest MSE when compared to other models, even for traits for which it had the best prediction accuracy. Relative differences between MSE from the best and worst model were lower for body weight traits (BW10, BW15 and BW20) and higher for CHOL and INSUL.

TABLE 2

Impact of feature selection on prediction performance

Figure 3 shows the prediction accuracy obtained by GBLUP, ENET and GBM when fitting only the top 100, 250, 500, 1000 from a GBM run or all SNPs (52K). When compared to fitting all SNPs (SNPALL), fitting only a subset of important features showed distinct pattern depending on the trait analyzed and model applied.

When fitting the GBLUP model, including increasingly more important SNPs resulted, for most traits, in an incremental increase in accuracy, reaching its maximum value in the SNPALL scenario. This was especially the case for traits which were expected to be highly polygenic like BW10, BW15, BW20 and FATP. For CHOL, GLUC and INSUL, fitting GBLUP with a subset of top importance SNPs selected by the GBM model yielded higher accuracy than SNPALL, the number of top SNPs that resulted in the highest prediction accuracy was dependent on the trait being analyzed.

When fitting ENET, including subsets of relevant SNP as predictors for BW10, BW15 and BW20 yielded similar results as for GBLUP. For FATP, there was an incremental increase in accuracy by including more important SNPs, but with SNP500 and SNP1000

showing even higher prediction accuracies than in SNPALL and comparatively higher than the accuracies obtained for FATP by GBLUP. For most other traits (except for BW10 and UCRT), fitting an ENET considering only some top SNPs showed higher prediction accuracies than SNPALL.

The GBM model showed for almost all traits a higher predictive accuracy when considering a subset of SNPs compared to fitting all available SNP (SNPALL). The only exception to that was UCRT, for which the inclusion of important SNPs up to 500 resulted in only a marginal increase in accuracy. For each tested subset of important SNPs, GBM outperformed GBLUP and ENET for prediction accuracy, except for FATP. For this trait, ENET yielded around 0.02 higher absolute accuracy than GBM for SNP1000. For BMD and UCRT, the total number of features selected by GBM was 364 and 419. Consequently, for these traits, running SNP1000 was not possible and SNP500 indicate SNP364 and SNP419, respectively.

FIGURE 3

Generation gaps and connectedness between reference and validation sets

Figure 4 shows the prediction accuracies obtained for different scenarios considering increasing distance between reference and validation sets. The increase in distance between the reference and validation sets resulted in a decrease in prediction accuracy for almost all trait/model combinations, in different magnitudes. The exception to that pattern was observed for GLU, for which a marginal increase in accuracy (although not drastically different across scenarios) was observed for GBLUP and GBM. Independent of the trait analyzed or model used, differences in accuracy between NoGAP and GAP9 were much lower than between NoGAP and GAP89 or between GAP9 and GAP89. These differences varied from - 0.20 (BMD – GBM) to +0.03 (GLUC – GBLUP).

The GBLUP model showed the lowest decrease in accuracy between NoGAP and GAP89 scenarios among traits when compared to other models, except for FATP, for which the difference in performance between NoGAP and GAP89 for GBLUP was the highest among all models (-0.12). On the other hand, the GBM model showed the highest drop in accuracy when comparing NoGAP and GAP89 scenario, especially for BMD, TRGL and UCRT. Especially for these traits, using GBM on a GAP89 scenario resulted in negative average prediction accuracies.

Independent of the model used, the traits BW10, BW15, BW20 and FATP showed the lowest decrease in accuracy while BMD, TRGL and UCRT showed the highest decrease in accuracy between NoGAP and GAP89 scenarios. For CHOL the prediction accuracy of GAP89 was higher than observed for GAP9 for all models tested, while for GLU this pattern was observed for predictions from GBLUP, BayesB and GBM, although in smaller differences between scenarios.

The ranking of model accuracy across traits observed using the full dataset (Figure 2) and for the generation gap scenarios (Figure 4) was not the same. When considering the full dataset, GBM yielded the best accuracy for BMD, CHOL and GLU, however the same pattern was not observed for the generation gap scenarios. Overall, when under any of the generation gap scenarios, GBLUP had the best accuracy across traits.

FIGURE 4

Animal predictions and SNP ranking similarities between models

The number of unique animals among the top 20 ranked using GBLUP, BayesB ENET and GBM models is shown in Figure 5 (top) for BW10 (A) and GLUC (B). Respectively for these two traits, the number of unique animals in the top 20 rank was 4 and 10 for GBLUP, 10 and 14 for BayesB, 7 and 9 for ENET; and 7 and 11 for GBM. Detailed

results for all traits are included in Supplementary Material – Figure S2. Overall, the number of overlapping animals between pairs and triples of models was slightly higher for BW10 than for GLUC. The number of animals uniquely in common between any model and GBM varied between 0 and 4 for BW10 and between 0 and 3 for GLUC.

Figure 5 also shows the count of overlapping markers among the top 1000 ranked by the models investigated for BW10 (C) and GLUC (D). Overall, the number of overlapping markers between any pair of models was higher for BW10 than for GLUC. Within traits, higher values were usually observed for comparisons between two linear models than between a linear model and GBM, while the lowest overlap was observed between ENET and GBM; and between BayesB and GBM. Comparisons between GBLUP and any other model had more overlapping markers than between other models. The largest differences between values above diagonal and the respective comparison below diagonal were observed for comparisons between GBLUP and any other model, with values above the diagonal (GBLUP x other model) being considerably higher than values below the diagonal (other model x GBLUP).

FIGURE 5

DISCUSSION

In the present study we compared predictive performances of commonly applied linear methods (GBLUP, BayesB and ENET) and a non-parametric machine learning ensemble method (GBM) for GP of 10 complex phenotypes in the DO mouse population. Although the evaluation of feasibility of genomic selection in mice was not our focus, results of predictive accuracy can be used as a guide if selection is intended for this population. Currently, the mating scheme used for the DO population is a randomized outbreeding strategy (Churchill et al., 2012), however, being able to predict phenotypes could be useful if any directional selection is of interest in the future.

Accuracies of GP have been reported by previous authors in another mice population (Legarra et al., 2008; Lee et al., 2008). Overall results showed low to medium predictive accuracies, ranging from 0.10 to 0.65 depending on the trait analyzed and cross-validation strategy considered. Our results confirmed that the performance of genomic prediction methods seem to be highly dependent on the trait's genetic architecture. When analyzing the traits that are mostly polygenic (BW10, BW15, BW20, FATP and TRGL), linear models were able to outperform GBM in both the full dataset (Figure 1) and for scenarios with lower connectedness between reference and validation subsets (Figure 4). BayesB was the best model for the three BW traits and FATP, while GBLUP had the best results for TRGL. In a genome-wide study using data from the same population, Zhang et al. (2010) showed an absence of QTL with pronounced effects for TRGL, with mostly small effects detected for genome-wide markers. This could explain why GBLUP had better predictive performance than BayesB or ENET for this trait.

Among the ten traits analyzed, evidence of non-additive effects has been reported for BMD (Tyller et al. (2016), CHL (Stewart et al., 2010; Li and Churchill, 2010) and GLU (Stewart et al., 2010; Chen et al., 2017). Coincidently for these traits GBM showed a better predictive performance than the linear models in the full dataset. Based on their results in strawberry using convolution neural networks, Zingaretti et al. (2020) suggested that machine learning methods may outperform parametric and semi-parametric models when the epistatic component is relevant (proportionally to the additive genetic variance) and narrow-sense heritability is medium to low (below 0.35). This is roughly in line with our results for CHL (h^2 = 0.33), GLU (h^2 = 0.11) and BMD (h^2 = 0.39). Interestingly, in our results the superiority of predictive ability from GBM compared to the parametric models was higher for the trait with lower heritability (GLU) than for CHL and BMD. Low-heritability traits imply that a smaller portion of observed variance is explained by the additive component, and therefore, any other non-linear effects might explain proportionally more of the phenotypic variance than in high-heritability traits. This larger proportion of the phenotypic variance with

a non-linear origin can more easily be captured by the GBM model, increasing performance of the model for such traits. Overall, the observed ranking of model performance across anticipated trait architecture was in line with previously reported results. In a detailed simulation study, Abdolahi-Arpanahi et al. (2020) showed that for traits controlled by many QTL (1000) with only additive effects, GBLUP and BayesB outperformed any machine learning approach, while for traits controlled by a small number of QTL (100) with non-additive effects, GBM largely outperformed other parametric and non-parametric models. Note that in their study, traits were simulated with only additive or non-additive effects, which is not expected to be the case in real world situations. However, their results on these extreme cases, are a robust indication of what to expect from each type of genomic prediction model. The similarity between results obtained in the present- and the afore-mentioned studies are in line with the current knowledge of genetic architecture of the analyzed traits (Table 1).

The efficient built-in feature extraction from GBM enables pre-screening of SNPs (Lubke et al., 2013; Li et al., 2018); and, therefore, minimize the loss in accuracy when reducing the number of markers in a genotype panel. The performance of GBM on pre-selection of informative SNP markers varied across traits and models subsequently used for phenotype prediction. When considering the highly polygenic traits (BW10, BW15, BW20, FATP and TRGL), using pre-selected SNP markers generally decreased accuracy of GBLUP. However, for ENET and GBM, in certain situations a subset of pre-selected SNP tended to yield higher predictive accuracy than using the complete SNP panel (Figure 3). For traits with evidence of non-linear effects (BMD, CHL and GLU), a similar pattern was observed, with the difference that the use of subsets of markers more commonly resulted in higher predictive accuracy than when fitting the models with all available SNP. After pre-selection of informative markers, GBM showed the biggest gains in accuracy across traits and models, which is expected, since we used a GBM model to accomplish the former. Azodi et al. (2019) observed that feature selection (using the random forest method) notably

515 improved prediction accuracies when using artificial neural networks (ANN) in multiple plant
516 species. However, in their case, predictive accuracies using ANN were overall lower than
517 other models. Using data from Brahman cattle, Li et al. (2018) investigated the potential of
518 three different ensemble learning methods to pre-select SNPs and showed that GBLUP
519 accuracies using SNPs preselected with GBM in some cases were actually similar to
520 accuracies based on all SNPs. Together with our findings, the above-mentioned results
521 suggest that GBM can be used for pre-screening informative markers, even when further
522 genomic prediction is performed using traditional linear models, such as GBLUP. One
523 limitation of ours and all investigations found in literature is the focus in performing feature
524 selection and further fitting top relevant markers into univariate models. Further research is
525 needed to expand this from a univariate to multivariate approach for practical implementation
526 in genomic selection breeding programs.

527 Curiously, for UCRT the inclusion of pre-selected SNP (from 100 to 500) did not
528 affect predictive accuracy, which was similar across scenarios and models, but always lower
529 than using the full SNP panel. This may occur because the optimum number of informative
530 markers might be above 500 or just that GBM was not successful at pre-selecting
531 informative markers for this particular trait. A similar pattern was previously reported by
532 Azodi et al. (2019) when fitting different numbers of informative pre-selected markers into a
533 model for genomic prediction in sorghum. Authors observed low and stable prediction
534 accuracy (around 0.40) when using up to 5% of top markers, but a strong increase when
535 using more than 5% of top relevant markers, reaching up to 0.60 when using 80% of
536 available markers. We have replicated the feature selection of top 100, 250, 500 and 1000
537 SNPs using BayesB instead of GBM. Results suggest a superiority of GBM for pre-selecting
538 informative markers (Supplementary Material – Figure S1) as predictive accuracy across
539 traits was consistently lower when using BayesB compared to using GBM for the same task.

540 The size of the reference population and the strength of the connectedness between
541 reference and validation subsets have been shown to influence GP accuracies from linear

models (Habier et al., 2007; Wientjes et al., 2013; Liu et al., 2015). In terms of connectedness, maximizing predictive performance involves maximizing connectedness between reference and validation populations, while simultaneously minimizing connectedness within the reference population (Pszczola et al., 2012). Although extensive research has been done over this topic regarding traditional GP using parametric models, this is not the case for ML models. In addition to that, much has been discussed in literature about how “data-hungry” machine learning models could be. However, studies have not only shown no clear superiority of predictive performance from machine learning over parametric models when using large datasets (Bellot et al., 2018), but also good performance of the same machine learning models when using datasets of hundreds of individuals (Azodi et al., 2019; Zingaretti et al., 2020; Bargelloni et al., 2021). When compared to the predictive performance of linear models, GBM had competitive results for most traits and a superior performance for BMD, CHL and GLU when using the full dataset (Figure 2). However, this relatively good performance was not maintained for NoGAP, GAP9 and GAP89 scenarios that contained less data (Figure 4). This pattern was observed across all traits and scenarios and may indicate that using only 300 individuals in the reference subset affected more drastically the predictive performance of the GBM model than GBLUP, BayesB or ENET. Overall, the decrease in accuracy observed from NoGAP to GAP89 was also more severe for GBM than for other models. We hypothesize that this could happen because as the distance between reference and validation populations increases, the frequency of recombination events also increases between genotypes from individuals in the two subsets. As GBM implicitly fits SNPxSNP interactions, the increased number of recombinations will impair the accurate estimation of allele combinations and interactions.

The ultimate aim of genomic prediction in the breeding context is to make accurate selection decisions early in the animal’s life. Therefore, comparing the top ranked individuals between methods is a useful way to understand how different these are in practical terms. In the present study, independent of the trait analyzed, linear models shared many more

individuals among the top 20 best from the three models (GBLUP, BayesB and ENET) than with GBM. For GLUC, for which we expected non-additive effects, the similarity between rankings for linear models was lower, while the number of unique animals for a single model were higher. On the other hand, as we consider BW10 to be controlled mostly by additive effects, the absence of relevant non-additive effects is probably the cause of lesser differences between linear models and GBM regarding selection decisions.

We evaluated the overlap among top ranked SNP between the different models (Figure 5, Supplementary Material – Figure S3). One thing that must be acknowledged is that there are differences in the way each of the different models estimate the relevance of a single SNP. This may affect the comparison of the overlapping relevant genomic regions between methods for a certain trait. For the linear models, SNP relevance is based on changes observed at the phenotypic level by the change in allelic dosage (0,1,2), while for GBM a SNP is considered relevant when the inclusion of this SNP in the decision tree contributes to a reduction in prediction error, and this can be affected by other SNP also used in the same decision tree. On the other hand, when used for genomic prediction, these differences will impact the obtained genomic predictions and thereby indirectly impact selection decisions. Therefore, this simple comparison of SNP ranks is informative to understand the similarity of outcomes from different models.

The asymmetry of results obtained from the overlapping top ranked SNP between models can be seen comparing values below and above diagonals in Figure 5 (C and D). The strongest driver of the differences observed seems to be the ability of models to perform variable selection. When starting comparisons from GBLUP (first row above diagonals in Figure 5 - C and D), there were many SNP located in specific short genomic regions among the top 1000 ranked SNP for this model. Several top markers from GBLUP were in high LD with at least one top ranked marker from the other models. In contrast, the variable selection applied by BayesB, ENET and GBM, resulted in fewer SNPs within a given genomic region to be among the top ranked ones. As a consequence, the number of top ranked SNP in high

LD with top ranked SNPs from the other models was much lower. Therefore, the difference between values above and below diagonal are directly related to the difference in magnitude of penalization applied to markers between any given pair of models. When comparing results from genomic prediction of height in maize using BayesA, ENET and random forest models, Azodi et al. (2019) have observed marked dissimilarity among the top 8000 markers. Results showed that BayesA and ENET shared 1589 (20%) markers, while RF shared 328 (4%) markers with BayesA and 475 (6%) with ENET. In the present study, this higher similarity among SNP ranks between linear models in addition to much lower similarity between linear models and an ensemble machine learning model (random forest in Azodi et al. [2019] or GBM in the present study) was also observed for BW10. At the same time, the difference between average SNP overlaps between two linear models or between a linear model and GBM was much lower for GLUC. From these results we can hypothesize that linear models have similar SNP rankings for polygenic traits because the underlying genetic architecture is in line with assumptions and parametrization considered in such models, while the presence of non-linear effects is probably captured differently by the distinct linear models, generating the observed overall dissimilarity.

CONCLUSION

Gradient boosting machine had a competitive performance for genomic prediction of complex phenotypes in mouse specifically for traits with non-additive effects where it can outperform linear models. The gradient boosting machine was more affected by datasets with less data points and by decrease in relationship between reference and validation populations than linear models. Considerable differences between the top ranked animals suggest that using linear models versus GBM will result in clear differences in selection decisions. The built-in feature selection from GBM seems beneficial to extract a smaller number of informative markers and in some cases can improve accuracies even when parametric models are used for prediction.

FUNDING

This project received funding from the European Union's Horizon 2020 research and innovation programme under grant agreement no. 817998.

REFERENCES

Abdollahi-Arpanahi, R., Gianola, D., and Peñagaricano, F. (2020) Deep learning versus parametric and ensemble methods for genomic prediction of complex phenotypes. Genet. Sel. Evol. 52, 12, https://doi.org/10.1186/s12711-020- 00531-z.

Azodi, C.B., Bolger, E., McCarren, A., Roantree, M., de los Campos, G., and Shiu, S.H. (2019). Benchmarking algorithms for genomic prediction of complex traits. G3 (Bethesda) 9, 3691–3702, https://doi.org/10.1101/614479.

Bargelloni L., Tassiello O., Babbucci M., Ferraresso S., Franch R., Montanucci L., Carnier P. (2021). Data imputation and machine learning improve association analysis and genomic prediction for resistance to fish photobacteriosis in the gilthead sea bream. Aquaculture Reports, Volume 20, 100661. https://doi.org/10.1016/j.aqrep.2021.100661

Barrera-Saldaña, Hugo A. (2019). Origin of personalized medicine in pioneering, passionate, genomic research. Genomics, 112-1, January 2020, p. 721-728. doi:10.1016/j.ygeno.2019.05.006

Bhat, J.A., Ali, S.; Salgotra, R.K., Mir, Z.A.; Dutta, S., Jadon, V.; Tyagi, A., Mushtaq, M., Jain, N.; Singh, P.K., Singh, G.P., Prabhu, K.V. (2016). *Genomic Selection in the Era of Next Generation Sequencing for Complex Traits in Plant Breeding. Frontiers in Genetics, 7().* doi:10.3389/fgene.2016.00221

Boichard D., Ducrocq V., Croiseau P., Fritz S. (2016) Genomic selection in domestic animals: Principles, applications and perspectives. C R Biol. Jul-Aug;339(7-8):274-7. doi: 10.1016/j.crvi.2016.04.007. Epub 2016 May 13. PMID: 27185591.

Broman K.W., Gatti D.M., Simecek P., Furlotte N.A., Prins P., Sen Ś., Yandell B.S., Churchill G.A. (2018). R/qtl2: software for mapping quantitative trait loci with high-dimensional data and multi-parent populations. Genetics 211:495-502 doi:10.1534/genetics.118.301595

Calus, M.P.L. (2010). *Genomic breeding value prediction: methods and procedures. animal, 4(2), 157–.* doi:10.1017/S1751731109991352

Canty A., Ripley B.D. (2021). *boot: Bootstrap R (S-Plus) Functions*. R package version 1.3-28.

Chitre, A.S., Polesskaya, O., Holl, K., Gao, J., Cheng, R., Bimschleger, H., Garcia M., Angel; G.T., Gileta, A.F., Han, W., Horvath, A., Hughson, A., Ishiwari, K., King, C.P., Lamparelli, A., Versaggi, C.L., Martin, C., St. Pierre, C.L., Tripi, J.A., Wang, T., Chen, H., Flagel, S.B., Meyer, P., Richards, J., Robinson, T.E., Palmer, A.A., Solberg W., Leah C. (2020). *Genomeâ€• Wide Association Study in 3,173 Outbred Rats Identifies Multiple Loci for Body Weight, Adiposity, and Fasting Glucose. Obesity, (), oby.22927.* doi:10.1002/oby.22927

Churchill G.A., Gatti D.M., Munger S.C., Svenson K.L. (2012). The Diversity Outbred mouse population. Mamm Genome. 2012 Oct;23(9-10):713-8. doi: 10.1007/s00335-012-9414-2. Aug 15. PMID: 22892839; PMCID: PMC3524832.

Click, C., Lanford, J., Malohlava, M., Parmar, V., and Roark, H. (2016). *Gradient Boosted Models with H2O*. http://docs.h2o.ai/h2o/latest-stable/h2o-docs/booklets/GBMBooklet.pdf.

Davison, A.C., Hinkley, D.V. (1997). *Bootstrap Methods and Their Applications*. Cambridge University Press, Cambridge. ISBN 0-521-57391-2, http://statwww.epfl.ch/davison/BMA/.

687 Duncan, L., Shen, H., Gelaye, B. *et al.* (2019) Analysis of polygenic risk score usage and
688 performance in diverse human populations. *Nat Commun* **10,** 3328.
689 https://doi.org/10.1038/s41467-019-11112-0

690 Forsberg S.K.G., Bloom J.S., Sadhu M.J., Kruglyak L., Carlborg Ö. (2017) Accounting for
691 genetic interactions improves modeling of individual quantitative trait phenotypes in yeast.
692 Nat Genet. 2017;49:497–503

693 Freund, Y., Schapire, R., & Abe, N. (1999). A short introduction to boosting. *Journal-*
694 *Japanese Society for Artificial Intelligence*, *14*(771-780), 1612.

695 Friedman J.H. (2001). Greedy function approximation: a gradient boosting machine. Ann
696 Statist.; 29:1189–232.

697 Friedman, J. H. (2002). Stochastic gradient boosting. Computational statistics & data
698 analysis, 38(4), 367-378.

699 Friedman, J.H. & Meulman, J.J. (2003). Multiple additive regression trees with application in
700 epidemiology. Statistics in Medicine, 22, 1365–1381.

701 Friedman J, Hastie T, Tibshirani. (2010). R: Regularization paths for generalized linear
702 models via coordinate descent. Journal of Statistical software, 33:1-22

703 Gatti D.M., Svenson K.L., Shabalin A., Wu L.Y., Valdar W., Simecek P., Goodwin N., Cheng
704 R., Pomp D., Palmer A., Chesler E.J., Broman K.W., Churchill G.A. (2014). Quantitative trait
705 locus mapping methods for diversity outbred mice. G3 (Bethesda). Sep 18;4(9):1623-33. doi:
706 10.1534/g3.114.013748. PMID: 25237114; PMCID: PMC4169154.

707 Ghafouri-Kesbi F., Rahimi-Mianji G., Honarvar M., Nejati-Javaremi A. (2016) Predictive
708 ability of Random Forests, Boosting, Support Vector Machines and Genomic Best Linear
709 Unbiased Prediction in different scenarios of genomic evaluation. *Animal Production*
710 *Science* **57**, 229-236.

711 González-Recio O.; Jiménez-Montero J.A.; Alenda R. (2013). *The gradient boosting*
712 *algorithm and random boosting for genome-assisted evaluation in large data sets. 96(1).*
713 doi:10.3168/jds.2012-5630

714 González-Recio O., Rosa G.J.M., Gianola D. (2014). *Machine learning methods and*
715 *predictive ability metrics for genome-wide prediction of complex traits. Livestock Science,*
716 *166(), 217–231.* doi:10.1016/j.livsci.2014.05.036

717 Gonzalez-Recio O, Forni S. (2011). Genome-wide prediction of discrete traits using
718 Bayesian regressions and machine learning. Genet Sel Evol., 43:7.

719 Grinberg, N.F., Orhobor, O.I. & King, R.D.(2020). An evaluation of machine-learning for
720 predicting phenotype: studies in yeast, rice, and wheat. *Mach Learn* **109,** 251–277.
721 https://doi.org/10.1007/s10994-019-05848-5

722 Habier D., Fernando R. L. and Dekkers J. C. M. (2007). The Impact of Genetic Relationship
723 Information on Genome-Assisted Breeding Values. GENETICS December 1, 2007 vol. 177
724 no. 4 2389-2397; https://doi.org/10.1534/genetics.107.081190

725 Hastie, T., Tibshirani, R., & Friedman, J. (2009). *The elements of statistical learning: data*
726 *mining, inference, and prediction*. Springer Science & Business Media.

727 Hoerl A, Kennard R. (1970). Ridge Regression: Applications to Nonorthogonal
728 Problems. *TECHNOMETRICS* 1970;12:69–82

729 Howard, R., Carriquiry, A. L., and Beavis, W. D. (2014). Parametric and non-parametric
730 statistical methods for genomic selection of traits with additive and epistatic genetic
731 architectures. G3 (Bethesda) 4, 1027–1046. doi: 10.1534/g3.114.010298

732 Keller M.P., Rabaglia M.E., Schueler K.L., Stapleton D.S., Gatti D.M., Vincent M., Mitok K.A.,
733 Wang Z., Ishimura T., Simonett S.P., Emfinger C.H., Das R., Beck T., Kendziorski C.,
734 Broman K.W., Yandell B.S., Churchill G.A., Attie A.D. (2019). Gene loci associated with
735 insulin secretion in islets from non-diabetic mice. J Clin Invest. Jul 25;129(10):4419-4432.
736 doi: 10.1172/JCI129143. PMID: 31343992; PMCID: PMC6763251

737 Jiang, R., Tang, W., Wu, X. *et al.* (2009). A random forest approach to the detection of
738 epistatic interactions in case-control studies. *BMC Bioinformatics* **10,** S65.
739 https://doi.org/10.1186/1471-2105-10-S1-S65

740 Jiménez-Montero J.A.; González-Recio O.; Alenda R. (2013). *Comparison of methods for*
741 *the implementation of genome-assisted evaluation of Spanish dairy cattle. 96(1).*
742 doi:10.3168/jds.2012-5631

743 Lappalainen T., Scott A. J., Brandt M., Hall I.M.. (2019). Genomic Analysis in the Age of
744 Human Genome Sequencing. Cell, Volume 177, Issue 1, 2019, Pages 70-84.

745 Li, Bo; Zhang, Nanxi; Wang, You-Gan; George, Andrew W.; Reverter, Antonio; Li, Yutao
746 (2018). *Genomic Prediction of Breeding Values Using a Subset of SNPs Identified by Three*
747 *Machine Learning Methods. Frontiers in Genetics, 9(), 237–.* doi:10.3389/fgene.2018.00237

748 Li, R. H., & Churchill, G. A. (2010). Epistasis contributes to the genetic buffering of plasma
749 HDL cholesterol in mice. *Physiological genomics*, *42A*(4), 228–234.
750 https://doi.org/10.1152/physiolgenomics.00044.2010

751 Lubke, G. H., Laurin, C., Walters, R., Eriksson, N., Hysi, P., Spector, T. D., et al. (2013).
752 Gradient boosting as a SNP Filter: an evaluation using simulated and hair morphology
753 data. *J. Data Min. Genomics Proteomics* 4:143. doi: 10.4172/2153-0602.1000143

754 Mackay, T., Stone, E. & Ayroles, J. (2009) The genetics of quantitative traits: challenges and
755 prospects. *Nat Rev Genet* 10**,** 565–577. https://doi.org/10.1038/nrg2612

756 Mackay, T.F.C. (2014). Epistasis and quantitative traits: using model organisms to study
757 gene–gene interactions. Nat Rev Genet. 2014; 15:22–33.

758 Meuwissen, T.H., Hayes B.J., and Goddard M. E. (2001) Prediction of total genetic value
759 using genome-wide dense marker maps. Genetics 157: 1819–1829.

760 Montesinos-López, O.A., Montesinos-López, A., Pérez-Rodríguez, P. *et al.* (2021). A review
761 of deep learning applications for genomic selection. *BMC Genomics* 22**,** 19.
762 https://doi.org/10.1186/s12864-020-07319-x

763 Moore K.J., Nagle D.L. (2000). Complex trait analysis in the mouse: The strengths, the
764 limitations and the promise yet to come. *Annu Rev Genet*. 34:653-686.

765 Morgan A.P., Fu C.P., Kao C.Y., Welsh C.E., Didion J.P., et al. (2016). The Mouse
766 Universal Genotyping Array: from substrains to subspecies. G3 (Bethesda) 6: 263–279.
767 10.1534/g3.115.022087

768 Nayeri S., Sargolzaei M., Tulpan D. (2019) A review of traditional and machine learning
769 methods applied to animal breeding. Anim Health Res Rev. 2019 Jun;20(1):31-46. doi:
770 10.1017/S1466252319000148. PMID: 31895018.

771 Neves, H.H., Carvalheiro, R. & Queiroz, S.A. (2012). A comparison of statistical methods for
772 genomic selection in a mice population. *BMC Genet* **13,** 100. https://doi.org/10.1186/1471-
773 2156-13-100

774 Pérez P. and de los Campos G. (2014) Genome-wide regression and prediction with the
775 BGLR statistical package. *Genetics*.198(2):483-495. doi:10.1534/genetics.114.164442

776 Pszczola, M., T. Strabel, H. A. Mulder, and M. P. L. Calus. (2012). Reliability of direct
777 genomic values for animals with different relationships within and to the reference
778 population. J. Dairy Sci. 95(1):389-400.

779 Rau C.D., Parks B., Wang Y., et al. (2015). High-Density Genotypes of Inbred Mouse
780 Strains: Improved Power and Precision of Association Mapping. *G3 (Bethesda)*.
781 2015;5(10):2021-2026. Published 2015 Jul 28. doi:10.1534/g3.115.020784

782 Sackton TB, Hartl DL. (2016) Genotypic Context and Epistasis in Individuals and
783 Populations. *Cell.*, 166(2):279-287. https://doi.org/10.1016/j.cell.2016.06.047

784 Srivastava, S., Lopez, B.I., Kumar, H., Jang, M., Chai, H.H., Park, W., Park, J.E., Lim, D.
785 (2021). Prediction of Hanwoo Cattle Phenotypes from Genotypes Using Machine Learning
786 Methods. *Animals*, *11*, 2066. https://doi.org/10.3390/ani11072066

787 Stewart, T.P., Kim, H.Y., Saxton, A.M. *et al.* (2010) Genetic and genomic analysis of
788 hyperlipidemia, obesity and diabetes using (C57BL/6J × TALLYHO/JngJ) F2 mice. *BMC*
789 *Genomics* **11,** 713. https://doi.org/10.1186/1471-2164-11-713

790 Svenson K.L., Gatti D.M., Valdar W., Welsh C.E., Cheng R., Chesler E.J., Palmer A.A.,
791 McMillan L., Churchill G.A. (2012) High-resolution genetic mapping using the Mouse
792 Diversity outbred population. Genetics. Feb;190(2):437-47. doi:
793 10.1534/genetics.111.132597. PMID: 22345611; PMCID: PMC3276626.

794 Tyler A.L., Donahue L.R., Churchill G.A., Carter G.W.. Weak Epistasis Generally Stabilizes
795 Phenotypes in a Mouse Intercross. PLoS Genet. 2016 Feb 1;12(2):e1005805. doi:
796 10.1371/journal.pgen.1005805. PMID: 26828925; PMCID: PMC4734753.

797 Tyler A.L., Ji B., Gatti D.M., Munger S.C., Churchill G.A., Svenson K.L., Carter G.W. (2017).
798 Epistatic Networks Jointly Influence Phenotypes Related to Metabolic Disease and Gene
799 Expression in Diversity Outbred Mice. Genetics. Jun;206(2):621-639. doi:
800 10.1534/genetics.116.198051. PMID: 28592500; PMCID: PMC5499176.

801 Van Dijk A.D.J., Kootstra, G., Kruijer, W., de Ridder, D. (2021). Machine learning in plant
802 science and plant breeding. iScience 24, 101890, January 22.

803 Van Raden, P.M. (2008). Efficient methods to compute genomic predictions. J. Dairy Sci.
804 91:4414-4423. https://doi.org/10.3168/jds.2007-0980

805 Yang, H., J.R. Wang, J.P. Didion, R.J. Buus, T.A. Bell et al. (2011) Subspecific origin and
806 haplotype diversity in the laboratory mouse. Nat. Genet. 43: 648–655.

807 Wientjes, Y.C.J.; Veerkamp, R.F.; Calus, M.P.L. (2013). *The Effect of Linkage Disequilibrium*
808 *and Family Relationships on the Reliability of Genomic Prediction. Genetics, 193(2), 621–*
809 *631.* doi:10.1534/genetics.112.146290

810 Zhang W., Korstanje R., Thaisz J., Staedtler F., Harttman N., Xu L., Feng M., Yanas L.,
811 Yang H., Valdar W., Churchill G. A. and DiPetrillo K. (2012). Genome-Wide Association
812 Mapping of Quantitative Traits in Outbred Mice. G3: GENES, GENOMES, GENETICS
813 February 1, vol. 2 no. 2 167-174; https://doi.org/10.1534/g3.111.001792

814 Zou H, Hastie T. (2005). Regularization and variable selection via the elastic net. Journal of
815 the Royal Statistical Society B, 67:301-320

816 Zingaretti, L. M., S. A. Gezan, L. F. V. Ferrao, L. F. Osorio, A. Monfort, P. R. Muñoz, V. M.
817 Whitaker, and M. Perez-Enciso. (2020). Exploring deep learning for complex trait genomic
818 prediction in polyploid outcrossing species. Frontiers in plant science, 11: 25. Doi:
819 10.3389/fpls.2020.00025

820

821

822

823

824

825

826

827

828

829

830

831

832

833

834

835

836

837

838

839

840

841

842

843

844

845 **Table 1.** Number of available observations (N), estimated heritability, assumptions from
846 literature regarding the genetic architecture of the trait and references.

Trait	N	Heritability	Genetic Architecture	Reference
BMD	831	0.39	Evidence of epistatic effects	Tyller *et al.* (2016)
BW10	834	0.42	Highly polygenic	Tyller *et al.* (2017) Chitre *et al*. (2018)
BW15	829	0.34	Highly polygenic	Tyller *et al*. (2017) Chitre *et al*. (2018)
BW20	827	0.37	Highly polygenic	Tyller *et al*. (2017) Chitre *et al*. (2018)
FATP	831	0.44	Highly polygenic	Tyller *et al*. (2017)
CHOL	819	0.33	QTL with high effect Evidence of epistatic effects	Stewart *et al*., (2010) Li and Churchill (2010) Zhang *et al*. (2012)
GLUC	816	0.12	Evidence of epistatic effects	Stewart *et al*. (2010) Chen *et al*. (2017)
INSUL	820	0.21	QTL with high effect	Keller *et al*. (2019)
TRGL	820	0.29	Highly polygenic	Stewart *et al*. (2010)
UCRT	799	0.13	Highly polygenic Evidence of dominance effects	Perry (2019)

847 [1] Standard error was close to 0.08 for all traits.

848
849
850
851
852
853
854
855
856
857
858
859
860
861
862

Table 2. Prediction error (mean squared error) obtained from GBLUP, BayesB, ENET and GBM for 10 phenotypes analyzed in the diversity outbred mouse population. Per trait, the lowest values are indicated in bold.

Trait[1]	GBLUP	BayesB	ENET	GBM
BMD	0.886	0.929	0.904	**0.885**
BW10	**0.023**	0.029	0.025	0.024
BW15	**0.025**	0.030	0.026	0.025
BW20	**0.029**	0.033	0.030	0.030
CHOL	0.068	0.104	0.080	**0.066**
FATP	**0.486**	0.523	0.488	0.493
GLUC	0.054	0.061	0.056	**0.051**
TRGL	**1.339**	1.503	1.373	1.367
INSUL	**0.198**	0.261	0.233	0.202
UCRT	**0.019**	0.022	0.020	0.020

[1]*Bone mineral density at 12 weeks (BMD), Body weight at 10, 15 and 20 weeks (BW10, BW15 and BW20); circulating cholesterol at 19 weeks (CHOL), adjusted body fat percentage at 12 weeks (FATP), circulating glucose at 19 weeks (GLU), circulating triglycerides at 19 weeks (TRGL), circulating insulin at 8 weeks (INSUL) and urine creatinine at 20 weeks (UCRT)*

886 ## FIGURES DESCRIPTION

887

888 **Figure 1.** Graphical representation of the hyper-parameter tuning grid-search scheme
889 implemented to obtain the best GBM and ENET models.

890

891 **Figure 2.** Prediction accuracy, including standard errors, obtained from GBLUP, BayesB,
892 elastic net (ENET) and gradient boosting machine (GBM) for the traits: *bone mineral density*
893 *at 12 weeks (BMD), Body weight at 10, 15 and 20 weeks (BW10, BW15 and BW20);*
894 *circulating cholesterol at 19 weeks (CHOL), adjusted body fat percentage at 12 weeks*
895 *(FATP), circulating glucose at 19 weeks (GLUC), circulating triglycerides at 19 weeks*
896 *(TRGL), circulating insulin at 8 weeks (INSUL) and urine creatinine at 20 weeks (UCRT)*.

897

898 **Figure 3.** Prediction accuracy, including standard errors, for the analyzed traits for GBLUP
899 (top), ENET (mid) and GBM (bottom) fitting exclusively the top 100 (SNP100), 250
900 (SNP250), 500 (SNP500), 1000 (SNP1000) ranked by a gradient boosting machine (GBM)
901 model and fitting all SNPs (SNPALL). *Traits: Bone mineral density at 12 weeks (BMD), Body*
902 *weight at 10, 15 and 20 weeks (BW10, BW15 and BW20); circulating cholesterol at 19*
903 *weeks (CHOL), adjusted body fat percentage at 12 weeks (FATP), circulating glucose at 19*
904 *weeks (GLU), circulating triglycerides at 19 weeks (TRGL), circulating insulin at 8 weeks*
905 *(INSUL) and urine creatinine at 20 weeks (UCRT).*

906

907 **Figure 4.** Distribution of prediction accuracies (from 20 replicates) for scenarios including
908 progressive distance between reference and validation sets using GBLUP, BayesB, elastic
909 net (ENET) and gradient boosting machine (GBM) models. *Traits: Bone mineral density at*
910 *12 weeks (BMD), Body weight at 10, 15 and 20 weeks (BW10, BW15 and BW20); circulating*
911 *cholesterol at 19 weeks (CHOL), adjusted body fat percentage at 12 weeks (FATP),*
912 *circulating glucose at 19 weeks (GLUC), circulating triglycerides at 19 weeks (TRGL),*
913 *circulating insulin at 8 weeks (INSUL) and urine creatinine at 20 weeks (UCRT)*

914

915 **Figure 5.** (A and B) Venn diagrams showing the unique animals among the top 20 (above)
916 predicted values (10% of the validation subset) between models and (C and D) the number
917 of SNP markers in common or in high LD ($r^2 > 0.90$) among the top 1,000 SNP from GBLUP,
918 BayesB (BB), elastic net (ENET) and gradient boosting machine (GBM) for BW10 (A and C)
919 and GLUC (B and D). In C and D, values represent the overlap of SNP when Model_1 (y-
920 axis) is considered as reference. Traits: *Body weight at 10, weeks (BW10); circulating*
921 *glucose at 19 weeks (GLUC).*

922

923

924

925

926

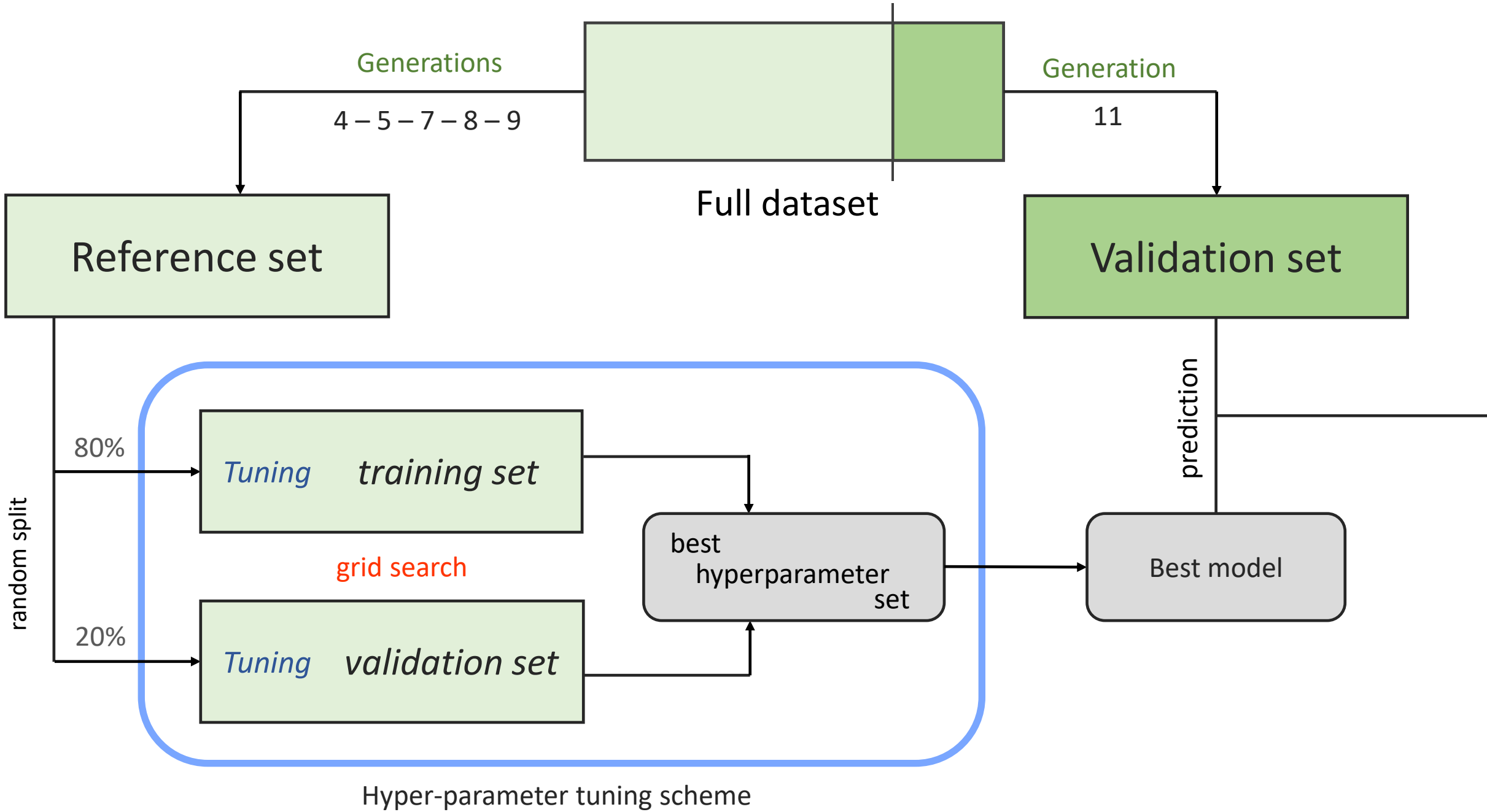
Generations
4 – 5 – 7 – 8 – 9
Generation
11
Full dataset
Reference set
Validation set
prediction
random split
80%
20%
Tuning training set
grid search
Tuning validation set
best hyperparameter set
Best model
Hyper-parameter tuning scheme

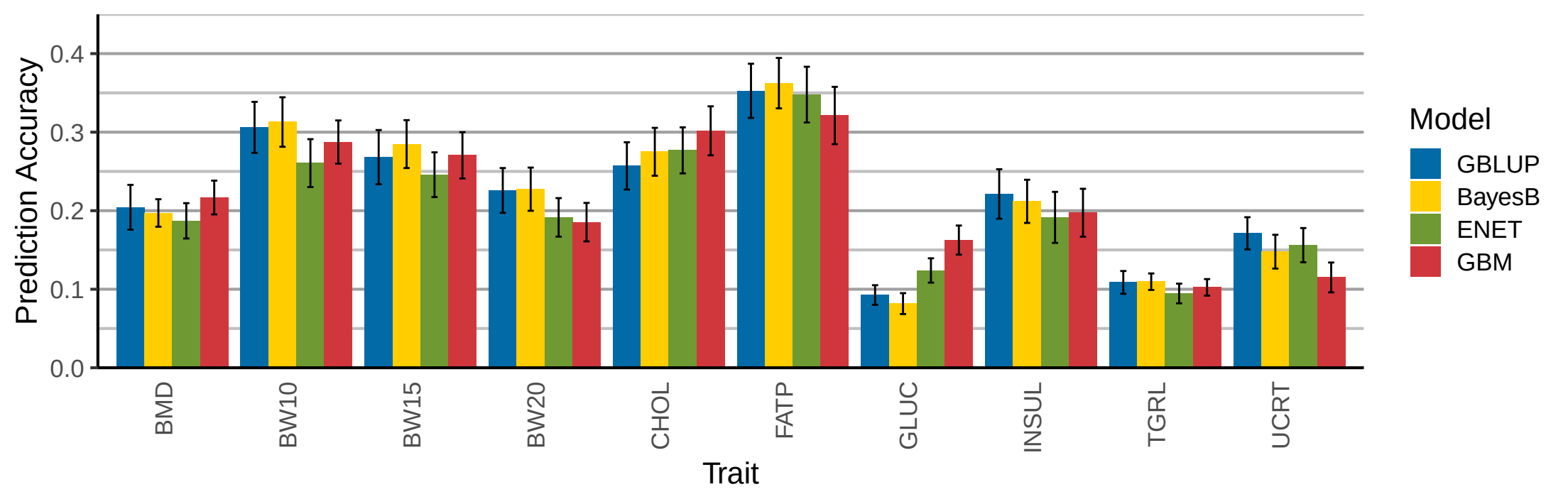
Prediction Accuracy
0.0
0.1
0.2
0.3
0.4
BMD
BW10
BW15
BW20
CHOL
FATP
GLUC
INSUL
TGRL
UCRT
Trait
Model
GBLUP
BayesB
ENET
GBM

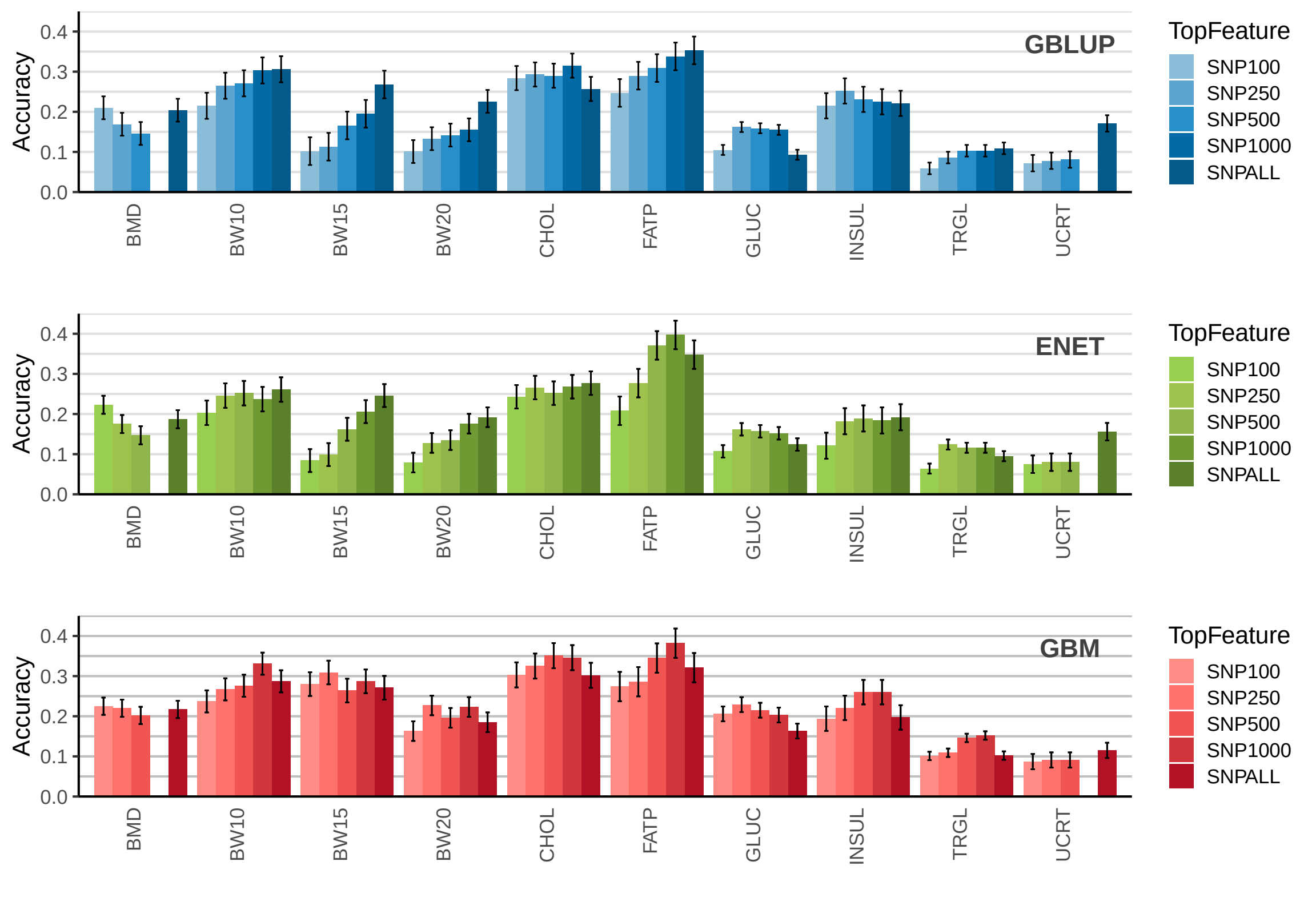
GBLUP
ENET
GBM
Accuracy
0.0
0.1
0.2
0.3
0.4
BMD
BW10
BW15
BW20
CHOL
FATP
GLUC
INSUL
TRGL
UCRT
TopFeature
SNP100
SNP250
SNP500
SNP1000
SNPALL

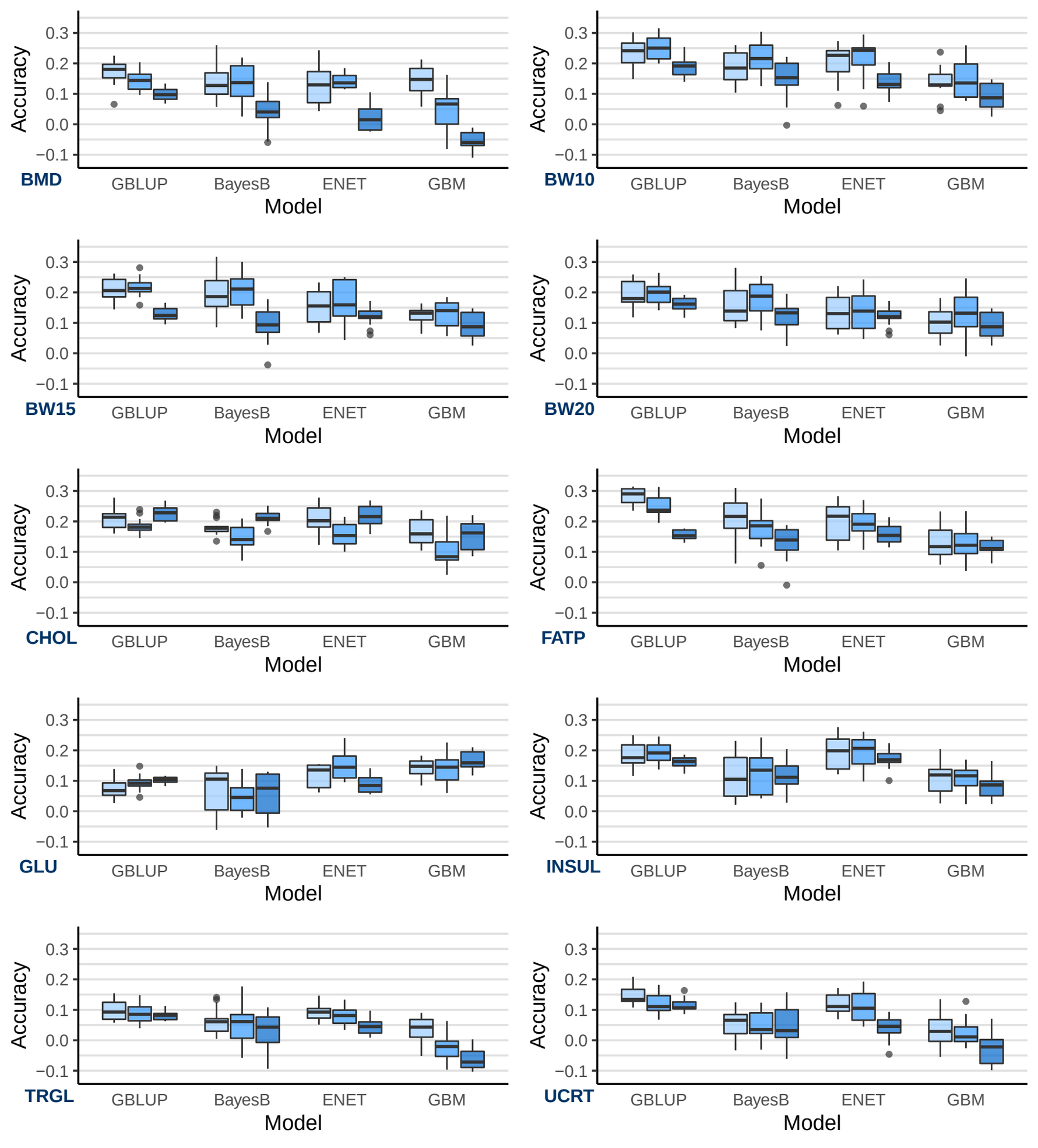
BMD
BW10
BW15
BW20
CHOL
FATP
GLU
INSUL
TRGL
UCRT
Accuracy
0.3
0.2
0.1
0.0
−0.1
GBLUP
BayesB
ENET
GBM
Model
Scenario
NoGAP
GAP9
GAP89

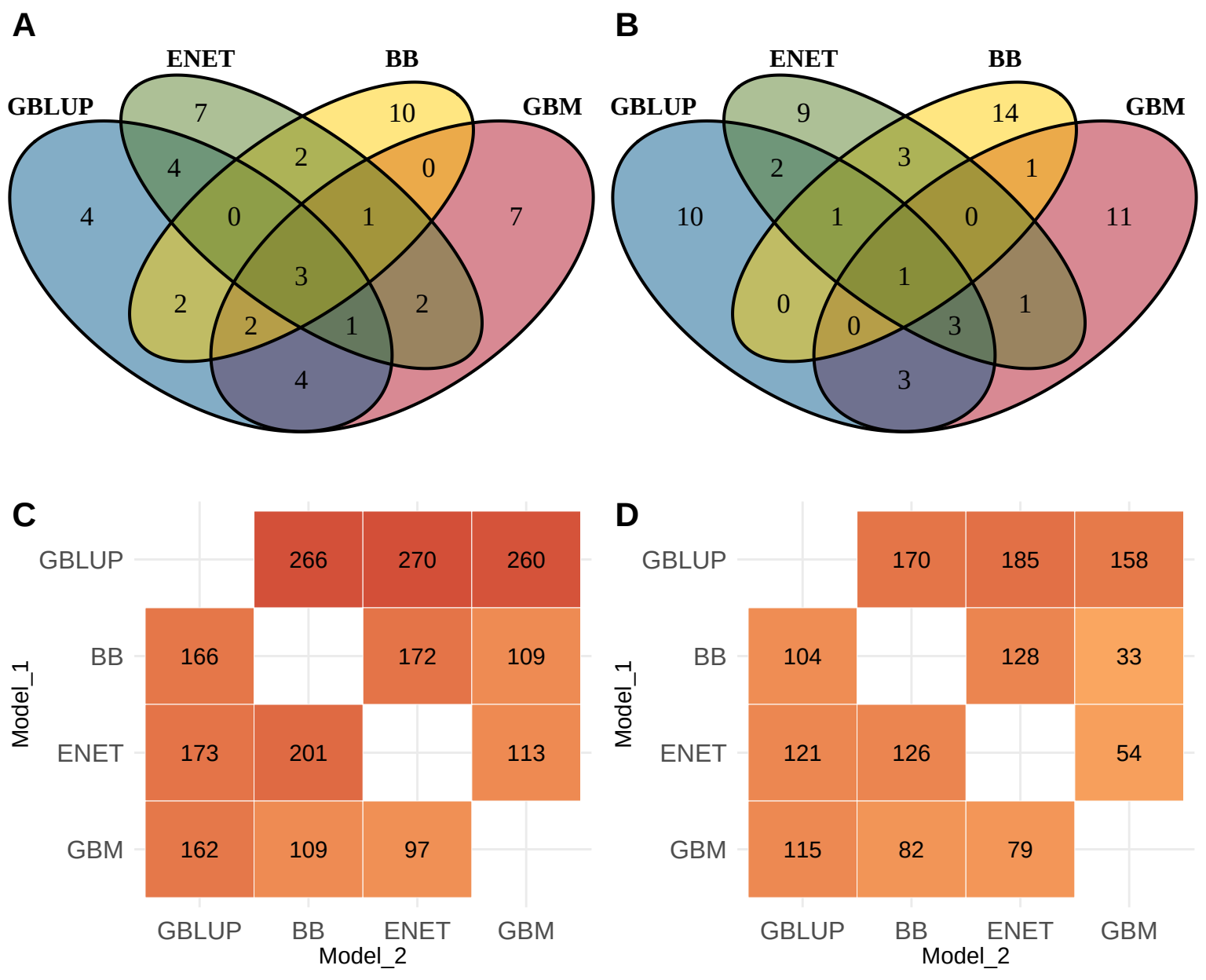
A
ENET
BB
GBLUP
GBM
7
10
4
2
0
4
0
1
7
3
2
2
2
1
4
B
ENET
BB
GBLUP
GBM
9
14
2
3
1
10
1
0
11
1
0
1
0
3
3
C
GBLUP
BB
ENET
GBM
Model_1
266
270
260
166
172
109
173
201
113
162
109
97
GBLUP
BB
ENET
GBM
Model_2
D
GBLUP
BB
ENET
GBM
Model_1
170
185
158
104
128
33
121
126
54
115
82
79
GBLUP
BB
ENET
GBM
Model_2